forests

MDPI

Article

The Effect of Tree-Uprooting on the Soil Spatial Complexity in an Old-Growth Temperate Forest, Central Europe

Andrea Román-Sánchez * and Pavel Šamonil

Department of Forest Ecology, The Silva Tarouca Research Institute, Lidická 25/27, 602 00 Brno, Czech Republic; pavel.samonil@vukoz.cz
* Correspondence: o92rosaa@uco.es

Abstract: The formation of spatial pedocomplexity in forested landscapes is an issue that has not yet been comprehensively resolved. This study analysed the effects of tree disturbances on the spatial variability of soil chemical properties in order to explain the spatial pedocomplexity in one of the oldest forest reserves in Europe. A total of 1545 sites over an area of 74 ha were assessed in terms of soil taxonomy, morphology, and profiles. We quantified the spatial autocorrelation of soil chemical properties and analysed the effects of soil disturbance regimes on soil chemical properties in both the surface and subsurface layers using geostatistics and redundancy analysis, respectively. A paired difference test revealed that the factors involved in the soil formation of the two layers are different. The neoformation of the surface layer proceeds rapidly after soil disturbance and, therefore, some formerly disturbed surface layers become mature above immature subsurface layers. The effect of tree disturbances on soil chemical properties was significant for totally decomposed treethrows. Treethrow density partially explained the variation in soil chemical properties in both layers, but even more so in the subsurface layer. This study further elucidates the impact of treethrows on soils and shows that they are an important driver of soil spatial pedocomplexity.

Keywords: soil spatial variability; geostatistics; soil evolution; podzolisation; Central Europe; tree–soil interactions

check for updates

Citation: Román-Sánchez, A.; Šamonil, P. The Effect of Tree-Uprooting on the Soil Spatial Complexity in an Old-Growth Temperate Forest, Central Europe. *Forests* **2022**, *13*, 769. https://doi.org/10.3390/f13050769

Academic Editor: John Campbell

Received: 2 March 2022
Accepted: 10 May 2022
Published: 17 May 2022

Publisher's Note: MDPI stays neutral with regard to jurisdictional claims in published maps and institutional affiliations.

Copyright: © 2022 by the authors. Licensee MDPI, Basel, Switzerland. This article is an open access article distributed under the terms and conditions of the Creative Commons Attribution (CC BY) license (https://creativecommons.org/licenses/by/4.0/).

1. Introduction

The spatial variability of soil properties has been investigated in many studies [1–5]; however, only a few studies have directly focused on the contribution of tree uprooting to soil spatial complexity [6,7].

Soil complexity can be described within a framework of the convergence and divergence evolution from two general perspectives. Regarding evolutionary pathways, such convergence or divergence leads to increasing or decreasing variability, diversity and irregularity over time. Concerning the perspective of soil complexity in general, complexity is related to spatial variability, pedodiversity, pedometrics, conceptual models of pedogenesis and soil geography, as well as evolutionary pathways [8]. Soils formed by a convergent trajectory may switch to divergent development due to climatic, geomorphic, tectonic, ecologic, and/or anthropomorphic disturbances [8]. Therefore, both convergence and divergence are closely related to dynamical instability and chaotic dynamics [9,10]. Several studies have revealed the crucial role of local disturbances (i.e., tree uprooting) in soil evolution in Western Europe [11], as well as in hillslope processes in some specific temperate ecosystems (e.g., mountain mixed Central European or North America forests [12–14]). Some authors have also suggested the potential significance of uprooting in soil spatial complexity in forested areas [15,16]. Despite efforts to explore the influence of treethrows in soils, little is known about the formation of spatial pedocomplexity in forested landscapes.

Podzols predominate in many temperate mountain forests and several theories describe the process of Podzol formation, i.e., podzolisation [17–19]. At the site studied here,

in the Žofinský Prales Reserve, Czech Republic, one process that is thought to be specially important is podzolisation, which involves the relocation of organo-mineral complexes from the top layer to the subsoil layer through eluviation and illuviation. In addition to Podzols, Dystric and Haplic Cambisols are also present in this area, although to a lesser extent than Podzols. In Cambisols, transport by leaching of organo-mineral complexes is not as important as in Podzols. Cambisols are composed of acid materials with a clay formation from primary minerals in a diagnostic cambic subsurface layer, as well as by its initial destruction by beginning podzolisation in the threshold surface and subsurface layers. The diversity of soil types and spatial pattern in the Žofinský Prales Reserve has not yet been sufficiently explained and we hypothesize that these variations are associated with tree disturbances caused by treethrows.

Explaining the spatial pedocomplexity of soil properties in old-growth forests and revealing the effect of tree disturbances in soil formation are important for a deeper understanding of geomorphological processes and landscape evolution. Our study helps address this topic by evaluating the effect of treethrows on soil formation using field data on associated soil chemical properties. The aim of this work was to analyse the effect of tree disturbances produced by treethrows on the spatial variability of soil chemical properties in the surface and subsurface layers, as well as on soil formation. This analysis attempted to explain the soil spatial pedocomplexity in one of the oldest forest reserves in Europe. To achieve this goal, we (i) differentiated soil chemical properties according to their source (external and pedogenic), (ii) used geostatistical methods to quantify the soil spatial variability, and (iii) applied multivariate statistical techniques to assess the effect of tree disturbances on soil formation processes.

2. Materials and Methods

2.1. Site Description

The study was conducted in the Žofínský Primeval Forest Reserve (hereinafter referred to as Zofin), located in the Novohradské Mountains in the SW Czech Republic (48°39′58″ N, 14°42′28″ E). The core zone of Zofin has been strictly protected since 1838, and is the fourth oldest forest reserve in Europe. Zofin belongs to the ForestGeo global network of forest research plots (www.forestgeo.si.edu/ (accessed on 20 January 2021)), and was the first such site in continental Europe. We studied soils in an area of 74.2 ha at an altitudinal range of 745–822 m a.s.l., with slopes of an average steepness of 8.6°. Regarding aspect, all directions are present in the study area, but with very little incidence to the south and southeast (Figure 1). The mean annual precipitation total is 866 mm, and mean annual temperature is 6.2 °C. Under the Köppen–Geiger system [20], the climate can be classified as Dfb (humid continental climate). The geology is composed of fine to medium-grainy porphyritic and biotite granite. The main vegetation is composed of a natural spruce-silver fir-beech forest, although the proportions of *Picea abies* and especially *Abies alba* have been decreasing due to air pollution, strong windstorms, and bark beetle outbreaks in the past few decades. The dominant soils in terrestrial areas are Entic Podzols and to a lesser extent Albic Podzols and Haplic and Dystric Cambisols (Figure S1) [7]. Only rarely do soils have additional layers between the surface and subsurface (such as E, Bhs, Bsg, or Bm). In areas around streams and other sites strongly affected by water, which cover about one third of the area, there are hydromorphic and semihydromorphic soils, specifically Histic and Haplic Gleysols, Haplic Fluvisols, and Endogleyic Stangonosols of the FAO-Unesco World Reference Base [21,22].

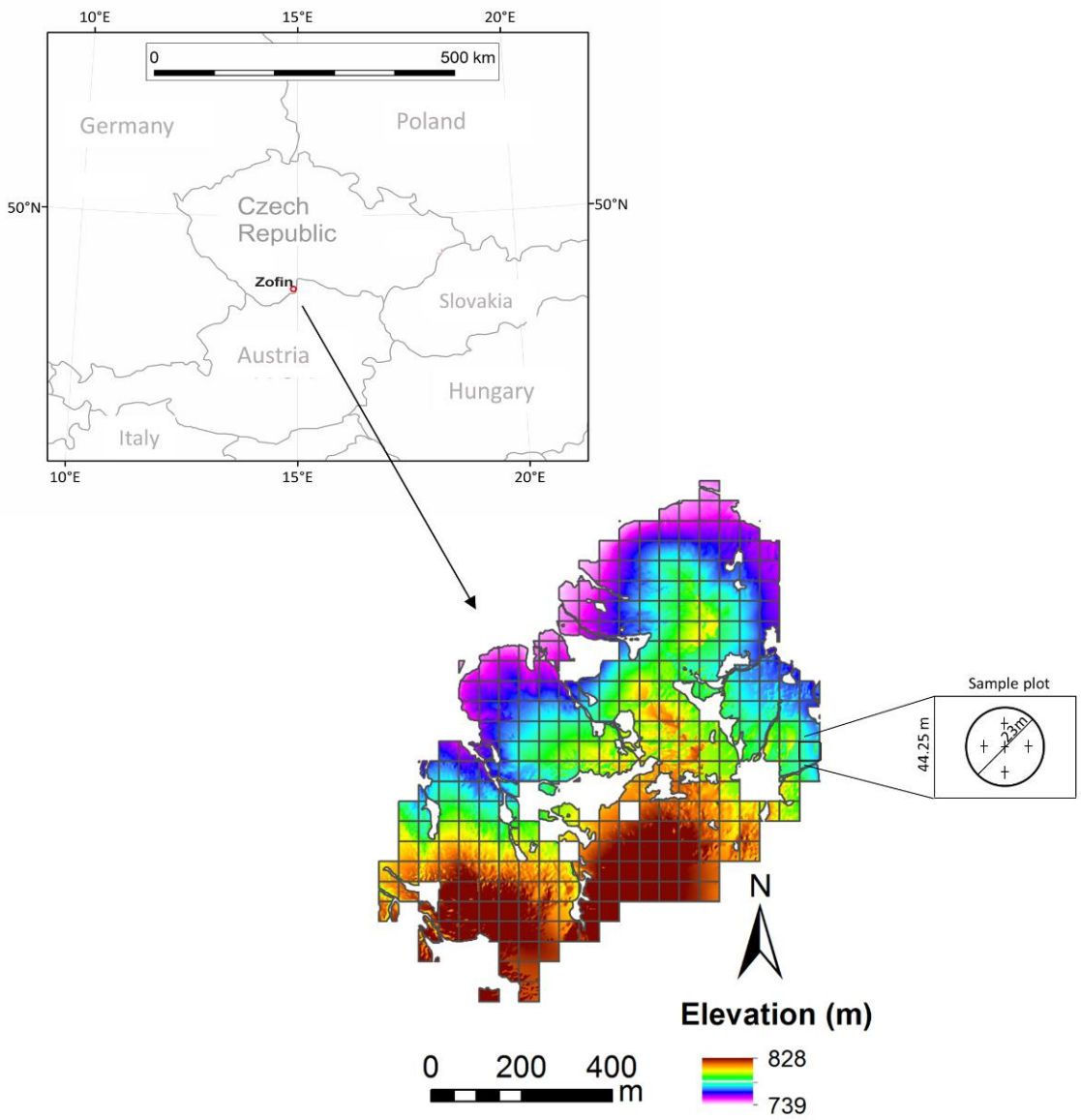

Figure 1. Location and elevation of the study area, and the sampling methodology. The black dots are the location of four soil profiles randomly selected in the study area. White areas represent soils with hydromorphic characteristics that were not considered in this study.

2.2. Soil Sampling and Analyses

The study area was divided into square grids of about 44 m (the distance was derived from the Czech Forest Inventory, www.uhul.cz (accessed on 20 January 2020)). In each square (309 in total), we identified a circle 23 m in diameter around the centre of each square. In these circles, five soil profiles were described in terms of soil morphology [23] and classified [21,22] (Figure 1), for a total of 1545 shallow soil profiles over the entire study area. Within each profile, we sampled the surface layer (0–15 cm) and the subsurface layer (15–60 cm). Then, the five samples from each layer within one square were mixed to obtain a representative sample per square. We thus obtained 309 mixed samples from the surface layer and 309 mixed samples from the subsurface layer. The surface and subsurface layers in each soil profile were distinguished during the field work. Generally, the surface layer coincided with horizon A (and horizon E in the case of Albic Podzols), with signs of eluviation and a higher content of organic matter, aggregates, roots, a darker colour, and with a higher porosity than the subsurface layer or horizon B. In addition, the B horizon showed signs of illuviation. Both horizons showed a clear boundary [24]. Soils

with hydromorphic characteristics were not considered in this study. We avoided sampling sites with treethrow pit-mound microtopography visible on the surface, but sites with lying trunks and levelled forms were included in our dataset (more details are given below). The samples were collected between 2010 and 2015.

The mixed fine earth sample from each square was analysed for 23 soil chemical properties. These were selected to best indicate the degree of soil evolution (with podzolisation being the most crucial soil forming process at the site) and plant nutrition. In addition, the same chemical properties and texture were analysed from the surface layer to below the subsurface layer in four soil profiles selected randomly in the study area: one in Albic, one in Entic Podzols, one in Haplic, and one in Dystric Cambisols (Figure S2). In the podzolic soils, nearly no clay was present, and the effect of organic matter predominated. In the soil profiles studied, we distinguished and assessed two aspects of soil properties based on expectations of their behaviour in soils and field measurements of soil chemical concentrations (Figure 2). First, we considered soil chemical properties of external sources (from complexes with organic matter or from parent material), which are characterized by decreasing concentrations with depth to the subsurface layer (Figure 2a,b). The soil chemical properties of external sources were considered to be: organic carbon (C_{ox}), determined spectrophotometrically after oxidation by H_2SO_4 + $K_2Cr_2O_7$, soil reaction (pH), exchangeable base cations of magnesium, calcium, sodium, and potassium (Mg^{2+}, Ca^{2+}, Na^{+}, K^{+}), aluminium cations (both interchangeable and the organically bound univalent, divalent, and trivalent aluminium species: Al $(X)^{1+}$, Al $(Y)^{2+}$, Al^{3+}), exchangeable acidity (EA), and the cation exchange capacity (CEC). The CEC represents the sorption capacity of soil, i.e., the total amount of exchangeable cations that the soil can absorb at the actual soil pH [25]. Note that the CEC has two important sources, organic matter and clay, but as mentioned above, because clay was nearly absent from these podzolic soils, the CEC is strongly driven by soil organic matter. Second, below the subsurface layer the soil chemical properties can increase with depth, depending on soil processes that occur in the soil profile or if the source is related to bedrock chemical weathering, as is the case for Ca^{2+}. We thus considered the soil chemical properties of pedogenic sources (formed by soil processes through the profile such as podzolization) as those that were characterized by increasing concentrations with depth until the lower part of the subsurface layer: exchangeable aluminium, manganese, and iron (Al_{KCl}, Mn_{KCl}, Fe_{KCl}), and aluminium, manganese, iron, and silicon oxides (Al_{ox}, Mn_{ox}, Fe_{ox}, Si_{ox}), Al_{dit}, Mn_{dit}, Fe_{dit}, Si_{dit} (Figure 2c,d). These soil chemical properties intervene in the podzolisation process, with the downward transport of complexes of organic acids and with Al and Fe, and the downward transport of Al and Si as inorganic colloidals [26].

In order to determine the biomechanical and biochemical interactions (tree disturbances) between tree uprooting and the spatial distribution of soil chemical properties and, therefore, whether spatial pedocomplexity is potentially associated with treethrows, we used a database of precisely determined stem positions of treethrows within the 23 m diameter circles of each square. This database, along with the identification of pits and mounds, was created in the study area between 2008 and 2013 (for details, see [27]). We distinguished three degrees of tree decomposition: totally decomposed—the trunk has already decayed and only the pit and mound microtopography exist at time of measurement; partly decomposed—a partly decomposed uprooted trunk is still present; and fresh treethrow—the uprooted tree trunk is still hard, without any decomposition. These forms were considered to be the youngest. In our study, soil samples were taken in apparently unmixed soil, so our assessment focused on the effect of tree disturbances on soil chemical properties. Tree disturbances occurred at Zofin during the Holocene period, from 1700 years ago to the present day [14]. The variables that were used in this study were treethrow density and treethrow depth (Table S1 and Figure S3). The treethrow depth was determined by measuring the depth of the roots when they were visible, or the depth of the pit when the tree was decomposed.

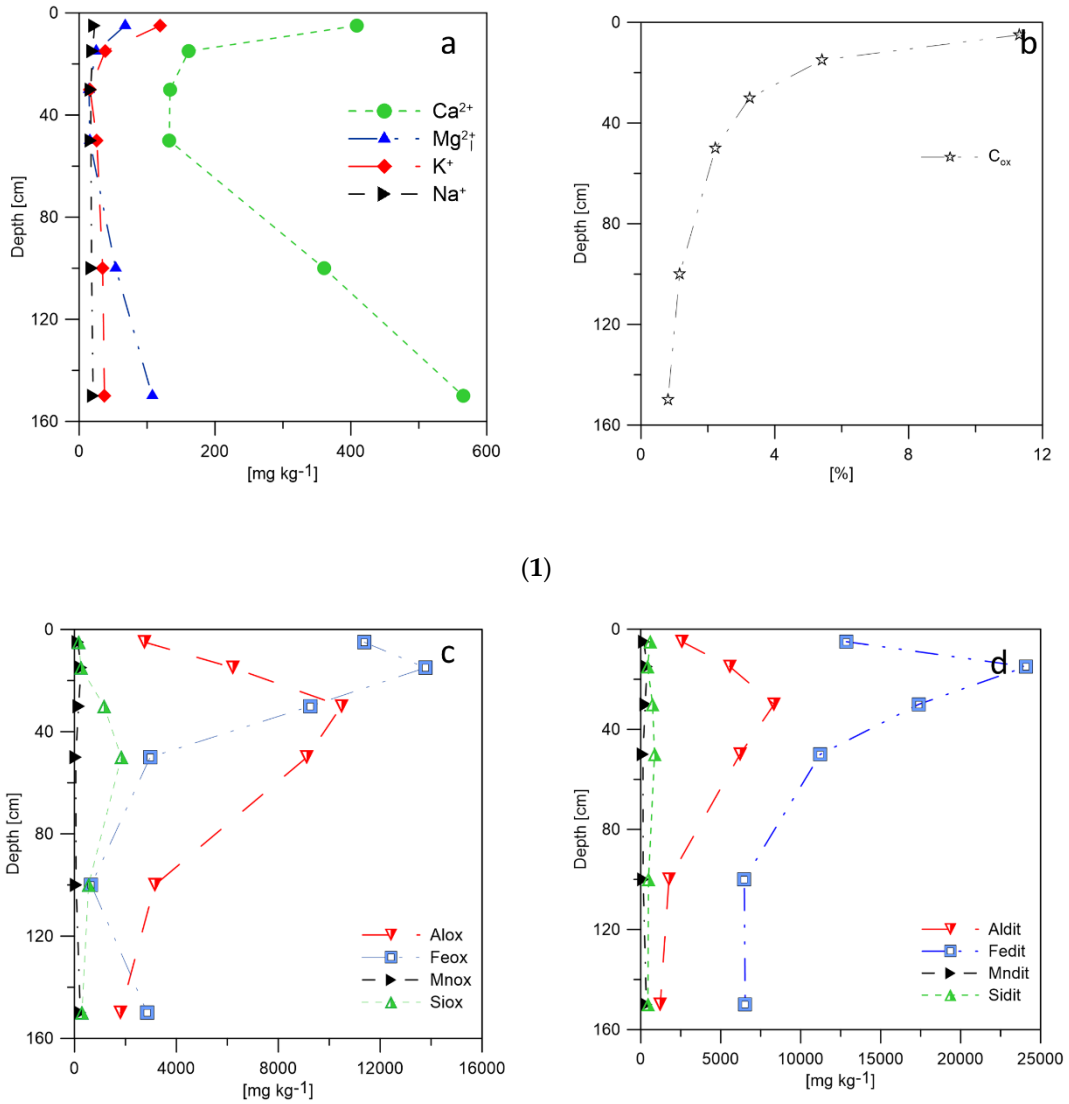

Figure 2. Vertical distribution in the soil profile of the soil chemical properties analysed in our study area. (**a**,**b**) were soil properties of external sources, and (**c**,**d**) were soil properties of pedogenic sources. (**1**). Soil chemical properties of external sources. (**2**). Soil chemical properties of pedogenic sources. Cations: Ca^{2+}-Calcium, Mg^{2+}-Magnesium, K^{+}-Potassium, Na^{+}-Sodium, Al_{ox}, Fe_{ox}, Mn_{ox}, Si_{ox}-Aluminium, Iron, Manganese and Silicon oxides, C-Carbon, Aldit, Fedit, Mndit, Sidit- Aluminium, Iron, Manganese and Silicon dithionite.

2.3. Statistical Data Analysis

2.3.1. Descriptive Statistics

According to the CV classification system proposed by [28], the soil chemical properties were classified as follows: A property was weakly variable if the CV was less than 10%, moderately variable if the CV was between 10% and 100%, and was otherwise strongly variable. An analysis of the linear correlation of Pearson coefficients (r) and p-values of the soil chemical properties was also performed.

2.3.2. Geostatistical Analysis

The geostatistical analysis to explore the spatial autocorrelation of the soil chemical properties was performed using Matlab R2021a. In linear geostatistics and statistics studies,

a normal distribution of variables is important from a methodological perspective [29]. In our study, several soil chemical properties showed considerable deviations from normality, and these variations could have affected the variogram results. First, the data normality of soil chemical properties of the surface and subsurface layer was tested with the Shapiro–Wilk test [30]. If the data did not follow a normal distribution, transformation with logarithmic, square root, or $1/x$ methods were performed (e.g., [31,32]). Then, omnidirectional experimental variograms were calculated by the following Equation (1):

$$\gamma\left(\vec{h}\right) = \frac{1}{2N}\sum_{i=1}^{N}\left[Z\left(\vec{x}+\vec{h}\right) - Z\left(\vec{x}\right)\right]^2, \quad (1)$$

where $\vec{x} = (x + y)$ denotes the coordinates of the centre of the elementary plot, $Z\left(\vec{x}\right)$ are the soil property values at $\vec{x}$ (or log or sqrt transformed values), $\vec{h}$ is a space separation vector, and N is the number of data pairs separated by $\vec{h}$.

Then, theoretical models that better fit the experimental variograms were calculated. The theoretical models tested were spherical, pentaspherical, circular, exponential, whittle, stable, and matern [33,34]. We used the Akaike Information Criterion (AIC) estimator to select the best-fitting theoretical model in each soil layer. From the theoretical models, all variogram parameters were calculated (range, sill, and nugget) using the ranges of these variograms as indicators of the maximum autocorrelation distance of the soil chemical properties (Figure S4). The next step was comparing the variogram parameters in each soil layer. Because a direct comparison of different models was not possible, we first selected the same fitted model for the surface and subsurface layer using the AIC estimator. Then, we applied a paired difference test, either a parametric (Student's t-test) [35] or non-parametric (Wilcoxon signed-rank test) [36] hypothesis test, depending on the distribution normality, with a confidence level of 95%.

2.3.3. Relationships between Treethrow Density and Treethrow Depth and Soil Chemical Properties

To explore the influence of treethrow on soil chemical properties, we analysed the relationships between treethrow density, treethrow depth, and soil chemical properties in both the surface and subsurface layer, as well as in the different soil units. We used the Pearson correlation coefficient (r) to evaluate relationships between variables, with significant relationships indicated with asterisks according to their significance level: *** $p < 0.001$; ** $p < 0.05$; * $p < 0.1$.

2.3.4. Redundancy Analyses

The effect of treethrow density and treethrow depth in the whole soil chemical properties dataset, both in the surface and subsurface layer, as well as in the different soil units, was investigated using redundancy analysis (RDA) as a multivariate technique. The RDA is a direct extension of regression analysis to model multivariate response data [37]. This analysis was performed using the vegan package 2.5–7 [38] in R 4.0.5 (R Core Team 2021). The RDA is based on Euclidean distances and performs linear mapping. Hellinger transformation was applied to standardize the soil chemical properties data with the decostand function. The explanatory variables considered were treethrow density and treethrow depth. To test the null hypothesis, which was that the explained variation in the dataset was produced by random chance, a Monte Carlo test with 10,000 permutations was applied. The null hypothesis was rejected if the p value was equal to or smaller than the predefined significance level ($\alpha = 0.05$).

3. Results

3.1. Descriptive Statistics

Despite the homogeneous geological bedrock in the study area, we found surprising richness of local soil types (Figure S1). In general, the forest contains acid soils, where the exchangeable pH ranged from 2.5 to 3.7 in the surface and 3.5 to 4.2 in the subsurface layer. Organic carbon ranged between 5% and 20% in the surface and between 1% and 6% in the subsurface layer, reflecting the expected decreasing content with soil depth (Table 1, Figure S5).

Table 1. Descriptive statistics of the surface and subsurface layers. Specifically, the descriptive statistics of the Podzols and Cambisols in the surface and subsurface layers are also shown (N = 309 samples for the surface and 309 samples for the subsurface layer). Additional information can be found in Table S2 in the Supplementary material.

Soil Chemical Properties	**Surface Layer**			**Subsurface Layer**		
	Mean	**Std. Dev**	**CV(%)**	**Mean**	**Std. Dev**	**CV(%)**
			External			
Cox (%)	9.4	2.2	23.6	2.8	0.7	25.2
$pH_{\_KCl}$	3.1	0.1	5.8	3.9	0.1	2.9
CEC (mmol(+)kg^{-1})	133.7	18.1	13.5	58.3	19.2	32.8
EA (mmol(+)kg^{-1})	130.2	23.2	17.9	54.9	14.3	26.0
Mg^{2+} (mg kg^{-1})	63.7	20.0	31.4	9.6	11.9	124.2
Ca^{2+} (mg kg^{-1})	0.3	0.2	66.6	0.3	0.1.	113.7
Na^{+} (mg kg^{-1})	13.6	8.6	63.8	13.0	8.8	67.2
K^{+} (mg kg^{-1})	112.6	29.1	25.9	21.8	12.0	55.1
$Al(X)^{1+}$ (mg kg^{-1})	118.6	25.6	21.6	14.6	3.7	25.3
$Al(Y)^{2+}$ (mg kg^{-1})	11.3	3.2	28.2	7.7	4.3	56.0
Al^{3+} (mg kg^{-1})	556.3	140.5	25.3	345.8	82.6	23.9
			Pedogenic			
AlKClsum	686.3	158.3	23.1	368.1	85.6	23.3
AlKCl (mg kg^{-1})	688.9	171.6	24.9	395.6	84.5	21.4
MnKCl (mg kg^{-1})	60.6	77.7	128.3	6.8	6.4	93.1
FeKCl (mg kg^{-1})	228.0	120.3	52.7	8.9	7.4	83.2
AlOx (mg kg^{-1})	4170.7	1006.5	24.1	12,201.9	4773.1	39.1
MnOx (mg kg^{-1})	140.6	161.5	114.9	198.4	182.9	92.2
FeOx (mg kg^{-1})	12,202.9	3559.7	29.2	12,296.0	3579.9	29.1
SiOx (mg kg^{-1})	246.8	125.5	50.9	1299.7	861.1	66.3
Aldit (mg kg^{-1})	3473.9	1083.3	31.2	8936.1	3502.7	39.2
Mndit (mg kg^{-1})	175.6	177.5	101.1	279.5	193.2	69.1
Fedit (mg kg^{-1})	18,039.2	4269.8	23.7	21,086.7	4563.1	21.6
Sidit (mg kg^{-1})	721.8	497.8	69.0	1198.5	603.5	50.4

Soil Chemical Properties	**Podzol**				**Cambisol**			
	Surface Layer		**Subsurface Layer**		**Surface Layer**		**Subsurface Layer**	
	Mean	**Std. Dev**	**Mean**	**Std. Dev**	**Mean**	**Std. Dev**	**Mean**	**Std. Dev**
				External				
Cox (%)	10.4	1.1	3.2	0.3	9.0	0.7	2.6	0.1
pH_{KCl}	3.1	0.1	4.0	0.0	2.9	0.1	4.0	0.0
CEC (mmol(+)kg^{-1})	128.0	6.1	67.4	8.5	134.3	1.7	54.8	0.8
EA (mmol(+)kg^{-1})	124.1	8.5	62.1	5.6	127.9	0.3	52.8	1.8
Mg^{2+} (mg kg^{-1})	53.4	6.6	6.1	3.0	68.0	3.7	11.5	2.1
Ca^{2+} (mg kg^{-1})	0.3	0.0	0.1	0.0	0.4	0.0	0.1	0.0
Na^{+} (mg kg^{-1})	16.5	4.1	11.6	0.6	12.6	2.2	14.9	2.2
K^{+} (mg kg^{-1})	106.8	5.1	16.8	2.1	117.8	2.5	24.9	1.1
$Al(X)^{1+}$ (mg kg^{-1})	107.7	12.8	17.1	1.4	112.3	3.4	13.1	0.4
$Al(Y)^{2+}$ (mg kg^{-1})	10.7	1.2	6.5	1.2	11.1	0.3	8.0	0.4
Al^{3+} (mg kg^{-1})	508.3	69.4	380.9	22.2	541.1	4.2	334.2	0.9
				Pedogenic				
Al_{KClsum}	626.7	82.9	404.5	23.4	664.5	0.5	355.3	0.1
Al_{KCl} (mg kg^{-1})	630.4	83.5	433.5	24.7	661.0	7.6	381.5	1.0
Mn_{KCl} (mg kg^{-1})	17.9	20.0	2.5	2.8	86.8	2.7	9.9	1.4
Fe_{KCl} (mg kg^{-1})	235.2	33.4	14.1	3.4	186.7	23.6	6.0	0.3
Al_{ox} (mg kg^{-1})	3469.8	769.2	17,057.0	3415.6	4318.2	373.0	10,384.0	537.1
Mn_{ox} (mg kg^{-1})	42.4	45.8	77.4	75.8	215.8	11.6	294.1	3.3
Fe_{ox} (mg kg^{-1})	9815.4	2469.5	11,730.2	773.5	12,083.4	401.2	11,804.0	30.5
Si_{ox} (mg kg^{-1})	150.9	99.5	2288.3	744.5	299.8	38.3	987.1	69.3
Al_{dit} (mg kg^{-1})	2927.1	585.8	11,803.4	2370.4	3526.1	32.6	7881.8	492.4
Mn_{dit} (mg kg^{-1})	57.4	49.4	177.4	75.4	257.5	10.0	371.8	2.7
Fe_{dit} (mg kg^{-1})	14,478.9	3345.5	21,502.6	988.1	18,060.1	901.4	20,523.5	45.2
Si_{dit} (mg kg^{-1})	696.2	100.8	1523.2	299.7	740.4	38.0	1148.8	37.6

Soil properties of an external source, such as C_{ox}, pH, CEC, EA, Mg^{2+}, Ca^{2+}, Na^{+}, K^{+} and Al cations, had higher mean values in the surface than in the subsurface layer. Of the aluminium cations, the largest proportion was the highly toxic Al^{3+}, representing an average 81% and 93% in the surface and subsurface layers, respectively. $Al(Y)^{2+}$ represented about 2% of the total in both layers, and the least-toxic species, $Al(X)^{1+}$, accounted for 17% and 4% in the surface and subsurface layers, respectively. Soil properties of pedogenic sources, Al_{ox}, Mn_{ox}, Fe_{ox}, Si_{ox}, Si_{dit}, Mn_{dit}, Al_{dit}, and Fe_{dit}, had higher mean values in the subsurface layer than in the surface or below the subsurface layer (Figure 2c,d). The differences in the content of amorphous forms of Mn and Fe were minimal in the surface and subsurface layers, but the Al content was three times higher and the Si content was five times higher in the subsurface layer. In contrast, Al_{KCl}, Mn_{KCl}, and Fe_{KCl} had higher mean values in the surface than in the subsurface layer.

For soil units, Podzols showed a higher organic carbon content than Cambisols in the surface and subsurface layers ($p = 0.01$ and 0.26, respectively). The contents of amorphous forms of Al, Mn, Fe and Si and Al_{dit}, Mn_{dit}, Fe_{dit} and Si_{dit} were higher in the Cambisols than in the Podzols in the surface ($p < 0.0001$). In contrast, the content of amorphous forms of Al, Fe, and Si and Al_{dit}, Fe_{dit}, and Si_{dit} were higher in the Podzols than in the Cambisols in the subsurface layer ($p < 0.0001$), with the minor exception of small differences in Mn_{ox}, Mn_{dit}, and Mn_{KCl} content between the two layers. These differences are most likely associated with cation exchange capacity (CEC), which was significantly higher in the Cambisols than in the Podzols in the surface layer and higher in the Podzols than in the Cambisols in the subsurface layer. Comparing the layers, the contents of amorphous forms of Al, Fe, and Si in the Podzols were higher in the subsurface than in the surface layer because of advanced pedogenesis, with minor exceptions for Mn. However, only the content of amorphous forms of Al and Mn were higher in the Cambisols in the subsurface than in the surface layer.

The coefficient of variance (CV) is an important indicator of the overall variation in the heterogeneity of soil chemical properties. The pH of both layers showed low variability (CV = 5.8 and 2.9%, respectively, for the surface and subsurface layers). In contrast, Mn_{KCl}, Mn_{ox}, and Mn_{dit} in the surface layer (CV = 128.3, 114.9 and 101.1%, respectively) and Mg^{2+} and Ca^{2+} in the subsurface layer (CV = 124.2 and 113.7%, respectively) showed strong variability. All other chemical soil properties had a CV ranging from 10 to 100%, suggesting moderate variability. When comparing the layers, the CV of soil chemical properties of external sources was higher in the subsurface layer, indicating a statistically significant higher heterogeneity of external soil chemical properties in the subsurface than in the surface layer. In the case of soil chemical properties of pedogenic sources, the CV was higher in the surface layer, suggesting a statistically non-significant higher heterogeneity of soil chemical properties of pedogenic sources in the surface than in the subsurface layer.

Regarding correlations, the relationships between soil chemical properties were stronger in the surface than in the subsurface layer, with higher correlation values (r) and higher significance levels (Figure 3). Specifically, the relationship of C_{ox} with soil chemical properties of external sources was positive and stronger in the surface than in the subsurface layer. The pH had negative and stronger relationships with soil chemical properties of external sources in the subsurface than in the surface layer. All forms of aluminium and pH were negatively related, and the relationships were stronger in the subsurface than in the surface layer. There were strong relationships between calcium, magnesium, and all forms of aluminium. Calcium and $Al(Y)^{2+}$ were positively related in both layers and the relationship was stronger in the subsurface than in the surface layer. $Al(X)^{1+}$ and Al^{3+} were negatively related to calcium, and the relationships were stronger in the surface than in the subsurface layer. Magnesium was positively related with $Al(Y)^{2+}$ and the relationship was very strong in both layers. In contrast, magnesium was negatively related to Al^{+3} and the relationship was stronger in the surface than in the subsurface layer. In the case of soil chemical properties of pedogenic sources, relationships with C_{ox} were negative and weak in the surface layer, but positive and strong in the subsurface layer. The soil chemical

properties of pedogenic sources, Mn_{ox}, Al_{ox}, Si_{ox}, Al_{dit}, Mn_{dit}, Fe_{dit}, and Si_{dit}, were all positively related to pH in both layers (Figure 3).

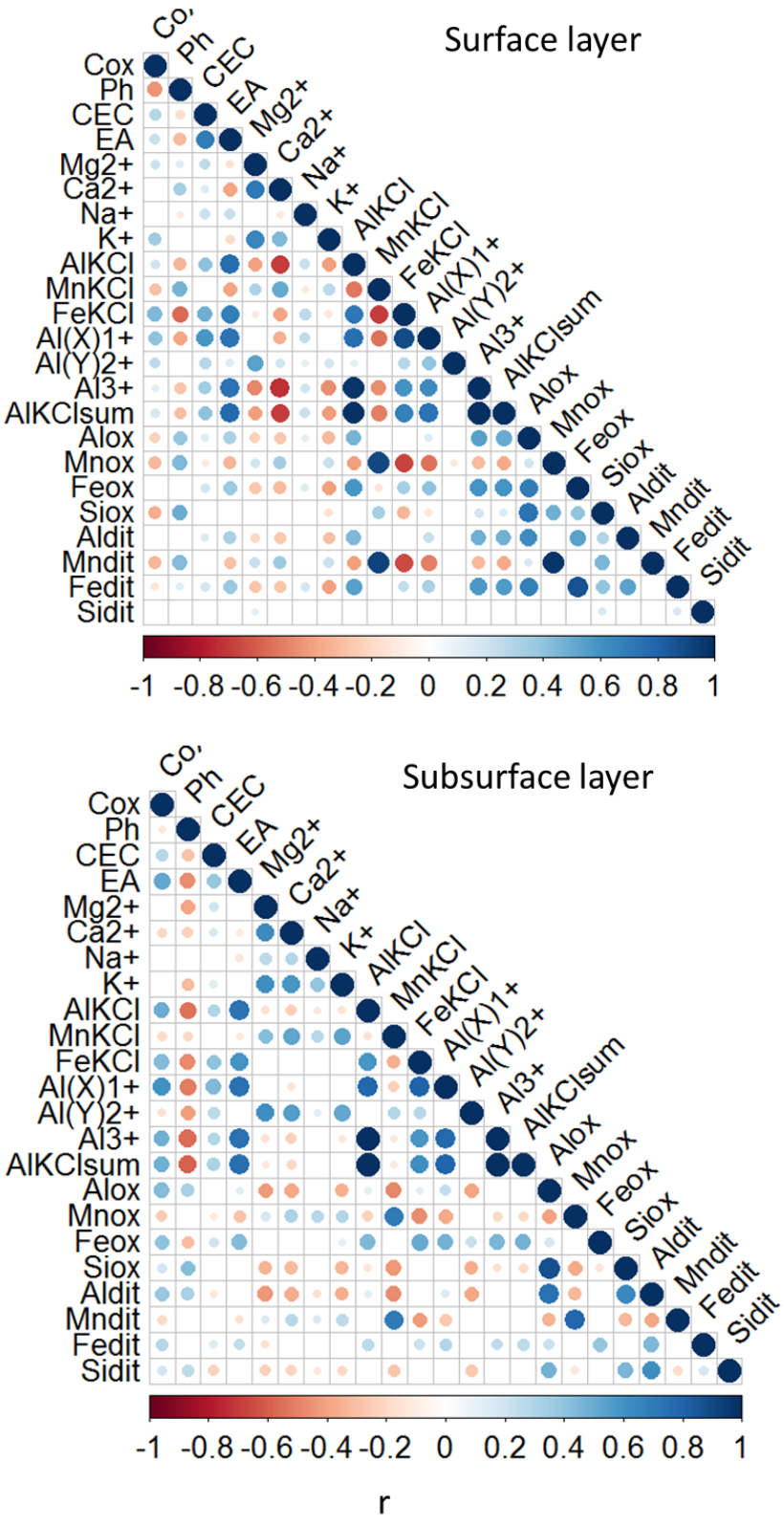

Figure 3. Pearson correlation coefficients for relationships between soil chemical properties for the surface and subsurface layers. Positive correlations are displayed in blue and negative correlations in

red. The colour intensity and the size of the circle are proportional to the correlation coefficients. Below and to the side of the correlogram, the legend colour shows the correlation coefficients and the corresponding colours. Correlations with *p*-value > 0.05 are considered insignificant, and the correlation coefficient values are left blank. Abbreviations: organic carbon (C_{ox}), soil reaction (pH), exchangeable base cations of magnesium, calcium, sodium, and potassium (Mg^{2+}, Ca^{2+}, Na^{+}, K^{+}), aluminium cations: Al $(X)^{1+}$, Al $(Y)^{2+}$, Al^{3+}, exchangeable acidity (EA), cation exchange capacity (CEC), exchangeable aluminium, manganese and iron (Al_{KCl}, Mn_{KCl}, Fe_{KCl}), aluminium, manganese, iron and silicon oxides (Al_{ox}, Mn_{ox}, Fe_{ox}, Si_{ox}) and Iron, Manganese and Silicon dithionite (Al_{dit}, Mn_{dit}, Fe_{dit}, Si_{dit}).

The texture of the Entic Podzols is mainly sandy in the upper and lower part of the profile, and loamy sand in some intermediate horizons, while the Albic Podzols have sand in the upper profile and loamy sand in the rest of the profile. The texture in the Haplic Cambisols is loamy sand in the upper and in intermediate horizons and sand in the bottom profile. The Dystric Cambisols are loamy sand in most of the profile and sandy loam in the lower part of the profile. Bulk density is lower in the Albic and Entic Podzols than in the Haplic Dystric Cambisols (Figure S6).

3.2. Spatial Patterns of Soil Chemical Properties

Generally, the results of the geostatistical analysis indicated that the exponential model was the best fit for most of the soil chemical properties in both layers (Table 2). Comparing the layers, the range values were generally higher in the surface than in the subsurface layer for most of the soil chemical properties. The highest values were for Na^{+} (103 m) in the surface layer and for CEC (254 m) in the subsurface layer. The lowest values were for Si_{dit} (31 m) in the surface layer and for Mg^{2+} (26 m) in the subsurface.

Table 2. Results of variograms parameters, range, sill, and nugget, and the statistical transformations of each soil chemical property (N = 309 samples for the surface and 309 samples for the subsurface layer).

	Surface Layer						Subsurface Layer				
	Model	**AIC**	**Effective Range**	**Sill**	**Nugget**		**Model**	**AIC**	**Effective Range**	**Sill**	**Nugget**
External						External					
Cox^{log}	Exponential	−110.68	52	0.05	0.00	Cox^{log}	Circular	−34.24	80	0.50	0.11
pH	Exponential	−137.91	59	0.00	0.00	Ph^{log}	Exponential	−179.88	165	0.02	0.01
CEC	Exponential	343.53	42	345.43	0.00	CEC^{log}	Circular	−84.67	254	0.06	0.07
EA	Exponential	329.66	39	584.07	0.00	EA^{log}	Spherical	−121.38	42	0.06	0.00
$Mg^{2+\,log}$	Exponential	−76.66	61	0.09	0.00	$Mg^{2+\,log}$	Gaussian	−5.11	26	0.44	0.00
$Ca^{2+\,sqrt}$	Gaussian	−157.16	132	0.03	0.02	$Ca^{2+\,log}$	Circular	−187.18	159	0.02	0.01
$Na^{+\,log}$	Gaussian	−25.55	103	0.171	0.122	$Na^{+\,log}$	Exponential	−19.98	70	0.27	0.00
$K^{+\,log}$	Exponential	−98.13	50	0.07	0.00	$K^{+\,log}$	Circular	−59.44	34	0.20	0.00
$Al(X)^{1+}$	Exponential	381.161	50	670.103	0.00	$Al^{1+\,log}$	Gaussian	−101.05	86	0.04	0.02
$Al(Y)^{2+\,log}$	Exponential	−94.75	45	0.07	0.00	$Al^{2+\,log}$	Exponential	−31.25	61	0.23	0.00
Al^{3+}	Exponential	556.43	46	20,068.31	0.00	$Al^{3+\,log}$	Exponential	−111.91	27	0.06	0.00
Pedogenic						Pedogenic					
Al_{KClsum}	Exponential	568.00	44	25,403.97	0.00	Al_{KClsum}^{log}	Circular	−120.12	42	0.06	0.00
Al_{KCl}	Exponential	576.26	47	29,209.92	0.00	Al_{KCl}^{log}	Circular	−126.81	42	0.05	0.00
Mn_{KCl}^{log}	Gaussian	103.22	99	2.50	0.60	Mn_{KCl}^{log}	Exponential	73.38	88	1.56	0.00
Fe_{KCl}^{log}	Exponential	0.53	48	0.45	0.00	Fe_{KCl}^{log}	Exponential	23.83	90	0.60	0.00
Al_{ox}^{log}	Exponential	−109.73	59	0.06	0.00	Al_{ox}^{log}	Exponential	−40.08	48	0.21	0.00
Mn_{ox}^{log}	Exponential	94.73	102	2.31	0.00	Mn_{ox}^{log}	Exponential	78.67	98	1.70	0.00
Fe_{ox}^{log}	Exponential	−72.03	53	0.11	0.00	Fe_{ox}^{log}	Exponential	−90.83	35	0.09	0.00
Si_{ox}	Exponential	507.16	73	15,894.54	2607.06	Si_{ox}^{log}	Exponential	7.11	44	0.53	0.00
Al_{dit}	Exponential	771.62	56	1175527.62	0.00	Al_{dit}^{sqrt}	Exponential	−35.38	50	0.22	0.00
Mn_{dit}^{log}	Exponential	249.49	80	2.40	0.37	Mn_{dit}^{sqrt}	Exponential	30.84	76	0.71	0.00
Fe_{dit}	Exponential	910.02	52	17,233,684.54	0.00	Fe_{dit}	Exponential	−110.34	41	0.06	0.00
Si_{dit}^{sqrt}	Exponential	98.72	31	3.28	0.00	Si_{dit}^{sqrt}	Exponential	26.41	55	0.71	0.00

In general, the soil chemical properties did not have a nugget effect, with a few showing a positive nugget effect (Na^{+}, Mn_{KCl}, Si_{ox} and Mn_{dit}) in the surface layer, and

C_{ox}, pH, CEC, Ca^{2+}, and Al^{1+} in the subsurface layer, explained by inherent variability (Liu et al., 2006).

Comparing soil chemical properties of external and pedogenic sources, we observed that the range values of soil chemical properties of external sources were generally lower in the surface layer than in the subsurface layer. In contrast, the range values were lower in the subsurface layer than in the surface layer for most of the soil chemical properties of pedogenic sources. Moreover, we found the highest range value for the soil properties of external sources in both layers (Na^{+} and CEC).

We applied the Wilcoxon signed-rank test (Wilcoxon, 1945) in the paired difference test for comparing the variogram parameters of both layers, because the data did not follow normality. The range and sill parameters indicated that the layers are significantly different (p-values < 0.05 = 0.041 and 0.020 respectively), while the nugget parameter indicated a non-significant difference between layers, with p-value > 0.05 = 0.161 (Table 3).

Table 3. Paired difference test (Wilcoxon signed-rank test) of variogram parameters between the surface and subsurface layer.

p-Value [1]		
Range	**Sill**	**Nugget**
0.041	0.020	0.161

[1] p-value < 0.05—significantly different; p-value > 0.05—not significantly different.

3.3. Relationships between Treethrow Density and Treethrow Depth and Soil Chemical Properties

Our field measurements in Zofin showed that the treethrow depth affected both the surface (0–15 cm) and the subsurface (~15–60 cm) layers, even though the mean value of the treethrow depth was 50 cm below the surface (Figure S7). In total, 42% of trees had roots shallower than 25 cm in depth, 34% of trees had roots between 25–55 cm, 20% of trees had roots between 55 and 100 cm, and 4% of roots were deeper, with a maximum value of 190 cm (data not published).

Concerning correlations, in the case of the totally decomposed treethrows, the treethrow density showed highly significant correlations with most soil properties of pedogenic sources in both layers, but even more significant relationships in the subsurface layer ($p < 0.05$, $p < 0.001$). Some soil properties of external sources (C_{ox}, EA, Mg^{2+}, Ca^{2+}, K^{+}, $Al(X)^{1+}$, $Al(Y)^{2+}$) showed significant correlations only in the subsurface layer ($p < 0.1$, $p < 0.05$). Comparing soil units, most soil chemical properties of pedogenic sources showed significant correlations only in the Entic Podzols in both layers, but with even more significant relationships in the subsurface layer ($p < 0.1$, $p < 0.05$, $p < 0.001$). No other important relationships were observed in the rest of the soil units. Generally, the significant correlations were negative in the surface layer, while some of the significant correlations were positive in the subsurface layer (Table 4).

In the case of partly decomposed treethrows, we found significant correlations between treethrow density and some soil chemical properties. For example, we observed significant correlations in Mg^{2+} and $Al(Y)^{2+}$ in the surface and CEC, and Al^{3+}, Al_{KClsum}, Al_{KCl}, and Fe_{dit} in the subsurface layers ($p < 0.05$, $p < 0.1$). Thus, we found more soil chemical properties with significant correlations in the subsurface layer than the surface layer. However, in the case of fresh treethrow, we did not observe important correlations between treethrow density and soil chemical properties (Table 5).

Regarding treethrow depth, in the case of totally decomposed treethrows, the treethrow depth showed significant correlations with some soil properties in the surface (C_{ox}, K^{+}, $Al(Y)^{2+}$) and subsurface layers (Mg^{2+}, Al_{ox}, Si_{ox}). Regarding soil units, we found some soil chemical properties with significant relationships only in the Dystric and Haplic Cambisols in the subsurface layer. For example, C_{ox}, pH, Mg^{2+}, and Al $(Y)^{2+}$ in Dystric Cambisols and Al_{ox}, Si_{ox}, Mn_{dit}, and Si_{dit} in Haplic Cambisols showed the most significant correlations ($p < 0.1$; $p < 0.05$) (Table 4). In the case of partly decomposed treethrows and fresh treethrows,

we did not observe significant correlations between treethrow depth and soil chemical properties (Table 5).

The significant relationships are indicated in Tables 4 and 5. All results in Tables 4 and 5 can also be found in the Supplementary Materials.

Table 4. Pearson correlation coefficient for the relationship between treethrow density and depth of treethrow and soil chemical properties for totally decomposed treethrow. Significant relationships are indicated in bold and marked according to their significance level: *** $p < 0.001$; ** $p < 0.05$; * $p < 0.1$. Note that the relationships shown in the table are significant for treethrow density and depth of treethrow. The soil units analysed are: AlPo-_Albic Podzol, EnPo-Entic Podzol, DyCa-Dystric Cambisol, HaCa-Haplic Cambisol. More information can be found in Table S3 in the Supplementary Materials.

Totally Decomposed Treethrow										
Treethrow Density										
Soil Properties	**Surface Layer**		**Subsurface Layer**		**Surface Layer**		**Subsurface Layer**			
					Soil Unit					
					EnPo		**EnPo**		**HaCa**	
External										
Cox	–		**0.15**	**	–		**0.17**	**	—	
pH	**−0.22**	***	—		**−0.16**	**	—		—	
EA	—		**0.10**	*	—		—		—	
Mg^{2+}	—		**−0.14**	**	—		—		—	
Ca^{2+}	—		**−0.10**	*	—		—		—	
Na^{+}	—		—		—		—		**−0.22**	*
K^{+}	—		**−0.14**	**	**0.17**	**	—		—	
$Al(X)^{1+}$	—		**−0.11**	*	—		—		—	
$Al(Y)^{2+}$	—		**−0.09**	*	—		**−0.17**	**	—	
Pedogenic										
Mn_{KCl}	**−0.17**	**	**−0.24**	***	**−0.15**	*	**−0.14**	*	**−0.22**	*
Al_{ox}	**−0.18**	***	**0.32**	***	**−0.14**	*	**0.33**	***	—	
Mn_{ox}	**−0.18**	***	**−0.23**	***	**−0.22**	***	**−0.17**	**	—	
Fe_{ox}	**−0.18**	***	—		**−0.2**	**	—		—	
Si_{ox}	**−0.21**	***	**0.27**	***	**−0.2**	***	**0.28**	***	—	
Al_{dit}	**−0.14**	*	**0.25**	***	—		**0.26**	***	—	
Mn_{dit}	**0.14**	***	**−0.20**	***	**−0.21**	***	**−0.19**	**	—	
Fe_{dit}	**−0.14**	**	**0.15**	**	–		**0.18**	**	—	

Totally Decomposed Treethrow										
Treethrow Depth										
Soil Properties	**Surface Layer**		**Subsurface Layer**		**Subsurface Layer**					
					Soil Unit					
					EnPo		**DyCa**		**HaCa**	
External										
Cox	**0.19**	***	-		-		**−0.43**	**	-	
pH	**-**		-		-		**−0.35**	*	-	
Mg^{2+}	**-**		**−0.11**	*	**-**		**−0.34**	*	-	
K^{+}	**0.12**	**	-		-				-	
$Al(Y)^{2+}$	**0.13**	**	-		-		**0.31**	*	-	
Pedogenic										
Al_{ox}	-		**0.16**	***	-		-		**0.25**	**
Si_{ox}	-		**0.13**	**	-		-		**0.27**	**
Mn_{dit}	-		-		-				**0.27**	**
Si_{dit}	-		-		**0.16**	*	**-**		**0.20**	*

Table 5. Pearson correlation coefficient for the relationship between treethrow density and depth of treethrow and soil chemical properties for partly decomposed treethrow and fresh treethrow. Significant relationships are indicated in bold and marked according to their significance level: *** $p < 0.001$; ** $p < 0.05$; * $p < 0.1$. Note that the relationships shown in the table are significant for treethrow density and depth of treethrow. More information can be found in Table S3 in the Supplementary Materials.

	Partly Decomposed Treethrow							
	Treethrow Density				**Treethrow Depth**			
	Surface Layer		**Subsurface Layer**		**Surface Layer**		**Subsurface Layer**	
External								
pH	-		-		-		**0.36**	**
CEC	-		**−0.41**	**	-		**−0.32**	*
Mg^{2+}	**0.37**	**	-		-		-	
$Al(Y)^{2+}$	**0.38**	**	-		**0.46**	***	-	
Al^{3+}	-		**−0.33**	*	-		-	
Pedogenic								
Al_{KClsum}	-		**−0.32**	*	-		-	
Al_{KCl}	-		**−0.35**	*	-		-	
Fe_{dit}	-		**−0.37**	**	-		-	
	Fresh Treethrow							
	Treethrow Density				**Treethrow Depth**			
	Surface Layer		**Subsurface Layer**		**Surface Layer**		**Subsurface Layer**	
External								
Cox	-		-		**0.17**	*	-	
Mg^{2+}	-		-		**0.20**	**	-	
K^{+}	-		-		**0.32**	***	-	
Pedogenic								
Mn_{KCl}	**−0.17**	*	-		-		**0.35**	***
Al_{ox}	-		-		**−0.18**	*	-	

3.4. Effects of Soil Disturbance Regimes on Soil Chemical Properties

In Section 3.3, we demonstrated the relationship between tree disturbances and soil chemical properties. In this section, we further investigate the effect of tree disturbances on soil chemical properties with a multivariate redundancy analysis. This analysis revealed that, for totally decomposed treethrows, treethrow density and treethrow depth explained 2.3 and 4.6% of the variation in soil chemical properties in the surface and subsurface layers, respectively. Regarding soil units, we found that the explanatory variables explained 4 and 6% of the variation in soil chemical properties only in the Entic Podzols in the surface and subsurface layers, respectively. In the case of partly decomposed treethrows, the explanatory variables explained 3.4 and 1.1% of the variation in soil chemical properties in the surface and subsurface layers, respectively. For fresh treethrows, the explanatory variables explained 2.1 and 1.1% of the variation in soil chemical properties in the surface and subsurface layer, respectively. In all cases of tree decomposition, most of the soil chemical properties of pedogenic sources and some soil properties of external sources, such as K^{+} and Al^{+3}, could be explained by the explanatory variables both in the surface and subsurface layers. The Monte Carlo permutation test with 10,000 random permutations showed that the model was highly significant for all categories of treethrow decomposition (p-value = 0.001) and both layers. For totally decomposed treethrows, treethrow density was highly significant ($p < 0.001$) in both layers ($n = 287$). Specifically, the treethrow density was significant ($p < 0.05$) in the Entic Podzols in both layers ($n = 140$). For partly decomposed

treethrows, treethrow density was significant ($p < 0.05$) in the subsurface layer ($n = 33$). In the case of fresh treethrows, none of the explanatory variables were significant ($n = 102$). However, depth of treethrow was not significant in any case (Table 6).

Table 6. Redundancy analysis (RDA). Pearson correlation coefficient for the relationship between treethrow density and treethrow depth, and soil chemical properties. No. samples indicates the number of plots in each category. Significant relationships are indicated in bold and marked according to their significance level: *** $p < 0.001$; ** $p < 0.05$. More information can be found in Table S4 in the Supplementary Materials.

Totally Decomposed Treethrow						
	Soil Layer	**No. Samples**	**No. Soil Properties**	**Explained Variability (%)**	***p*-Value**	**F-Value**
Treethrow density	Surface	288	23	2.3	<0.001 ***	6.31
	Subsurface	288	23	4.6	<0.001 ***	11.80
Entic Podzol						
	Soil Layer	**No. Samples**	**No. Soil Properties**	**Explained Variability (%)**	***p*-Value**	**F-Value**
Treethrow density	Surface	140	23	4	<0.05 **	2.82
	Subsurface	140	23	6	<0.05 **	6.21
Partly decomposed treethrow						
	Soil Layer	**No. Samples**	**No. Soil Properties**	**Explained Variability (%)**	***p*-Value**	**F-Value**
Treethrow density	Surface	34	23	3.4	>0.1	0.86
	Subsurface	34	23	1.1	<0.05 **	3.27

The significant relationships are shown in Table 6. All results in Table 6 and Figure S8 can also be found in the Supplementary materials.

4. Discussion

It is well known that soil is formed by a complex interaction of factors, including the parent materials, climate, relief, organisms, and time [39]. Although quantifying soil forming processes has been the goal of many studies [40–43], there is still a lack of knowledge in identifying and quantifying these processes, and they are usually not represented correctly in soil formation models [44]. In their review of the importance of soil processes in current landscape evolution models, [44] reviewed data and models on weathering rates, transport processes, soil profiles, and combined soil landscape evolution models, and discussed how scientists and modelers can work together in order to validate models with field data. They proposed 22 soil processes that need to be included in soil formation models (for example, podzolisation), but noted that only about 50% of these processes have been sufficiently studied to be used for this purpose. In our study, we attempted to elucidate the soil formation processes specific to podzolisation and the alteration of primary minerals into secondary (especially clay) minerals. Specifically, we (i) studied differences between the sources (external vs. pedogenic) of soil chemical properties, (ii) quantified and analysed the spatial variation in soil chemical properties in the surface and subsurface layers, and (iii) determined the effect of soil disturbance regime on soil chemical properties and on soil formation, to explain the soil spatial pedocomplexity in a natural temperate forest characterized by tree disturbances.

4.1. Vertical Patterns of External and Pedogenic Sources

Organic carbon content significantly moderates soil evolution in mountain soils on acidic granitic bedrock as in Zofin. This is related to the higher mean values of CEC and EA in the subsurface layer. Therefore, the main source of CEC comes from organic matter and not from clay, which is limited in podzolised soils. Calcium, magnesium, sodium, and potassium concentrations were higher in the surface than in the subsurface layer, associated with a higher amount of organic matter in the upper layer (Table 1). The natural distribution of calcium and magnesium can determine soil pH, which controls

the distribution of aluminium in soils, as demonstrated by [45]. Organic matter is also important in the distribution of aluminium, which is bound to organic complexes [46]. Soil acidity is closely linked with aluminium; lower pH is associated with higher risk of aluminium toxicity. Al^{+3}, associated with the mineral Al form, is related to phytotoxicity in acid soils, as discussed in detail by [47,48], and $Al(X)^{+1}$ and $Al(Y)^{+2}$ can bind to organic complexes. Therefore, the lower the pH, the higher the aluminium level and degree of plant toxicity. In addition, the acidification process is accelerated in soils occupied by *Picea abies*, such as at Zofin, as shown by [45].

The soil chemical properties of the external sources studied here generally had decreasing concentrations with sample depth. However, the trend for calcium with depth was the opposite, as similarly demonstrated by [49]. Calcium depends not only on humidity but also on the bedrock. Figure 2a shows that Ca^{+2} at our site had higher concentrations at the 150 cm depth than at the surface. Furthermore, the calcium concentration was lower in the subsurface than in the surface and in deeper layers. This distribution of calcium can be attributed to the fact that there are two sources of Ca^{+2}. Calcium is released from the bedrock by chemical weathering of feldspar, which is altered by hydrolysis to clay minerals. At the same time, calcium is derived from organic matter in the surface layer because in acid soils some minerals are completely dissolved and their components, including Ca^{+2}, go into solution. In addition, the uptake of cations by roots, mainly described for Fagus, influences the cation concentrations at the surface [50,51]. This highlights the fact that categorizing the source of soil chemical properties as external or pedogenic is difficult, due to the diverse sources of some soil chemical properties.

Regarding soil chemical properties of pedogenic sources, at our site amorphous forms were found in higher concentrations in the Podzols in the subsurface than in the surface layer, indicating an advanced pedogenesis process. Soil formation in the Cambisols was not as advanced as in the Podzols, i.e., the transport of amorphous forms was not as important.

4.2. Spatial Patterns of Soil Chemical Properties in the Surface and Subsurface Layer

In general, most of the soil chemical properties had a higher spatial autocorrelation in the surface than in the subsurface layer. Our findings are comparable to the results obtained in [7]. This can be explained by the effect of frequent uprooting, which has a lengthier effect in the subsurface compared to the surface layer, i.e., the formation of the subsurface layer requires more time than the formation of the surface layer. Tree uprooting processes have dominated in Zofin over the past thousands of years, and this may be considered an exceptional feature of the ecosystem dynamics (Figure 4). [52] found that hillslope dynamics are dominated by tree uprooting in Boubin (south Bohemian region, Czech Republic), which has similar ecosystems to Zofin and is in the same region, and [16] analysed the spatial pedocomplexity and its sources, including the effect of individual trees. Later, [14] demonstrated the long-term predominance of biogenic creep associated with tree uprooting in hillslope processes. Furthermore, the results obtained in the paired test indicated that the formation of both layers is different. We believe this reflects the effect of tree uprooting on soil chemical properties, as discussed above. Nevertheless, if we distinguish between external and pedogenic sources, we can interpret the spatial patterns of soil chemical properties as follows. The soil chemical properties of external sources had a higher spatial autocorrelation in the subsurface layer compared to the surface layer. The CV followed the opposite trend, with a higher CV for soil properties of external sources in the subsurface than in the surface layer. This finding is comparable to the study of [53]. This can be explained because the soil chemical properties of external sources are more affected by soil disturbances in the surface compared to the subsurface layer, of which formation is related to geology and topography.

Figure 4. Rock fragment extraction by an uprooted spruce. On the right is a notebook to compare the size of the roots and rock.

In contrast, the soil properties of pedogenic sources had a higher spatial autocorrelation in the surface than in the subsurface layer. The CV followed the opposite trend, i.e., it was higher in the surface than in the subsurface layer. This can be explained by the fact that the soil dynamics in the top are higher than in the subsurface layer. Therefore, the neoformation of the surface layer proceeds quite rapidly, and the disturbed top layer is developed above an immature subsurface layer. Furthermore, at our site, and as found in some other studies [54–56], Al_{KCl}, Mn_{KCl}, Fe_{ox}, Mn_{ox}, and Mn_{dit} concentrations in the topsoil are influenced by organic matter through reductions due to complexation reactions that increase with organic matter, and which depend on the CEC. Later, these soil chemical properties are translocated to the subsurface layer, as is inherent to a Podzol formation. However, Al_{KCl} and Mn_{KCl} are not transported in large amounts to deeper profile depths during podzolisation, as was also found in our study area.

4.3. Impacts of Tree Uprootings on Vertical and Spatial Patterns of Soil Chemical Properties

In a previous study on the old-growth temperate forest at Zofin, [15] detected a spatially non-random effect of tree uprooting on soil taxonomy. Here, we assessed the effect of treethrow disturbances on the vertical and spatial patterns of soil chemical properties, which are one of the drivers of soil spatial complexity. The influence of the treethrow density of totally decomposed treethrows is particularly important in podzolisation at our site. The treethrow density explained the higher variation in soil chemical properties of pedogenic sources in the Entic Podzols in both the surface and subsurface layers, but particularly in the subsurface layer. This indicates that the soil chemical properties are more affected by soil disturbances in the surface compared to the subsurface layer. In general, the negative correlation between treethrow density and the soil chemical properties of pedogenic sources in the surface layer denotes that these soil chemical properties in the surface are translocated to the subsurface layer. This relationship between treethrow density and soil chemical properties may also be interpreted as a link between the spatial pattern of disturbance regimes and soil patterns (see Section 4.2).

In summary, soil dynamics are likely to be higher in the surface than in the subsurface layer at our site. As demonstrated in our study, part of these dynamics is produced by tree disturbances, which is caused mostly by treethrow density of totally decomposed

treethrows in Entic Podzols. This scenario is likely to increase the organic matter content in soil and, as in forest soils, element cycling is strongly related to organic matter. Moreover, the dynamics of amorphous forms are determined by several factors, such as organic matter [54–56]. Therefore, it is likely that the organic matter content in the soil of the decomposed treethrows plays a fundamental role in the spatial and vertical distribution of soil chemical properties in Zofin. On the one hand, the treethrow density affects the vertical distribution of soil chemical properties in the soil profile, promoting podzolisation. Thus, these soil chemical properties are translocated to the subsurface layer, as discussed above. Hence, the neoformation of the surface layer after a soil disturbance proceeds rapidly, and the disturbed surface matures above the immature subsurface. On the other hand, tree disturbances intervene in the spatial distribution of soil chemical properties. This is also related to the spatial distribution of the soil carbon content. In fact, the differences in the spatial distribution of organic carbon are statistically significant between the totally decomposed treethrows areas and partly decomposed and fresh treethrow areas. In addition, the Entic Podzols have a lower bulk density in the surface layer due to the high organic matter content.

Future work is needed to identify and quantify the topographic and environmental factors that may control the spatial patterns of soil chemical properties. Additionally, it is potentially interesting to study the effect of the treethrow decomposition in soil weathering—biological, physical, and chemical. For example, it would be useful to quantify bioturbation using an analytical model based on luminescence techniques [43] or granulometry [57,58].

5. Conclusions

We demonstrated a moderate but significant effect of treethrows on the soil chemical properties in Zofin. This relationship between treethrow density and soil chemical properties may also be interpreted as a link between the spatial pattern of disturbance regimes and soil patterns. Treethrow density was the most significant explanatory variable for soil chemical properties, while treethrow depth was not significant. The treethrow density of totally decomposed treethrows explained the higher variation in soil chemical properties (4% in the surface and 6% in the subsurface layers) in the Entic Podzols. This can be explained by the fact that the soil chemical properties are more affected by the extremely frequent uprooting at the surface compared to the subsurface layer. Consequently, it is likely that the organic matter of the decomposed treethrows plays a fundamental role in the spatial and vertical distribution of the soil chemical properties at our site. On the one hand, treethrow density indirectly promotes podzolisation by allowing the translocation of the soil chemical properties from the surface to the subsurface layer, specifically amorphous forms, of which the dynamics are determined by organic matter at the surface. On the other hand, tree disturbances intervene in the spatial distribution of soil chemical properties. In fact, there are differences in the spatial distribution of soil organic carbon between areas with different degrees of treethrow decomposition. This highlights the impact of treethrows on soils, showing that they are one of the drivers of soil spatial pedocomplexity.

Supplementary Materials: The following supporting information can be downloaded at: https://www.mdpi.com/article/10.3390/f13050769/s1, Table S1: Treethrow density and treethrow depth. (a) Totally decomposed, (b) Partially decomposed and (c) Fresh treethrow; Table S2: (a) Descriptive statistics of the surface and subsurface layers. (b) The descriptive statistics are also shown for Podzols and Cambisols in the surface and subsurface layers. (N = 309 samples for the surface and 309 samples for the subsurface layer), Table S3: Pearson correlation coefficient for the relationship between treethrow density and depth of treethrow and soil chemical properties for totally and partly decomposed treethrow and fresh treethrow. Significant relations are indicated in bold and marked according to their significance level: *** $p < 0.001$; ** $p < 0.05$;* $p < 0.1$. Noted that the relations showed in the table are the significant in Treethrow density and Depth of treethrow. The soil unit analysed are: AlPo-_Albic Podzol, EnPo-Entic Podzol, DyCa-Dystric Cambisol, HaCa-Haplic Cambisol, Table S4: Redundancy analysis (RDA). Pearson correlation coefficient for the relationship between treethrow density and treethrow depth, and soil chemical properties. No. samples indicates the number of plots

in each category. Significant relations are indicated in bold and marked according to their significance level: *** $p < 0.001$; ** $p < 0.05$; * $p < 0.1$, Figure S1: The distribution of soil units in the study area. Entic Podzols (EnPo) were the most frequent soil unit, occupying 166 plots (47%). Dystric Cambisols (DyCa) and Haplic Cambisols (HaCa) were located in 138 plots (39%), and Albic Podzols (AlPo) were found in 30 plots (8%). The remaining plots had soils with significant amounts of stagnic, gleic, or even histic properties and/or horizons. Such soils were classified as Stagnosols (Sg), Gleysols (HHGl), Mix-d-mixed terrestrial soils (dry), and Mix-w-mixed (semi)-hydromorphic soils (wet). Note that hydromorphic soils and treethrows in them were not taken into account in this study. Figure S2: Soil profiles studied in the study area. Figure S3: Sampled treethrows in the study area in the three decomposition degrees: totally decomposed, partly decomposed, and fresh treethrow. Figure S4: Example of an experimental variogram fitted to an exponential model in the case of Al^{+2}. Figure S5: Boxplots of the soil chemical concentrations, both in the surface and subsurface layers, in the study area. Figure S6: Vertical distribution of bulk density in Haplic, Dystric Cambisols, and Albic and Entic Podzols. Figure S7: Histograms of treethrow depth measured in the study area. Figure S8: Redundancy analysis (RDA). Ordination diagram (triplot) showing the significant relationships of Table 6. Sites (denoted by points), explanatory variables (treethrow density and treethrow depth; red arrows), and response variables (soil properties; blue arrows). First axis is horizontal, second axis is vertical. The angles among arrows denote the degree of correlation between the individual variables; the smaller the angle, the larger the correlation. In addition, positively correlated variables are shown as arrows pointing in the same direction, while negatively correlated variables point in opposite directions.

Author Contributions: Conceptualization, A.R.-S. and P.Š.; methodology, A.R.-S. and P.Š.; software, A.R.-S.; validation, A.R.-S.; formal analysis, A.R.-S. and P.Š.; investigation, A.R.-S. and P.Š.; resources, P.Š.; data curation, A.R.-S. and P.Š.; writing—original draft preparation, A.R.-S.; writing—review and editing, A.R.-S. and P.Š.; visualization, A.R.-S.; supervision, P.Š.; project administration, P.Š.; funding acquisition, P.Š. All authors have read and agreed to the published version of the manuscript.

Funding: The research was supported by the Czech Science Foundation, project No. 19-09427S.

Data Availability Statement: Data are available on request from the corresponding author.

Acknowledgments: We thankfully acknowledge all our colleagues of Blue Cat team responsible for field surveys and sample processing.

Conflicts of Interest: The authors declare no conflict of interest.

References

1. Cambardella, C.A.; Moorman, T.B.; Parkin, T.B.; Karlen, D.L.; Novak, J.M.; Turco, R.F.; Konopka, A.E. Field-Scale Variability of Soil Properties in Central Iowa Soils. *Soil Sci. Soc. Am. J.* **1994**, *58*, 1501–1511. [CrossRef]
2. Gallardo, A. Spatial Variability of Soil Properties in a Floodplain Forest in Northwest Spain. *Ecosystems* **2003**, *6*, 564–576. [CrossRef]
3. Yanai, J.; Lee, C.K.; Umeda, M.; Kosaki, T. Spatial variability of soil chemical properties in a paddy field. *Soil Sci. Plant Nutr.* **2000**, *46*, 473–482.
4. Usowicz, B.; Lipiec, J. Spatial variability of soil properties and cereal yield in a cultivated field on sandy soil. *Soil Tillage Res.* **2017**, *174*, 241–250. [CrossRef]
5. Dai, W.; Li, Y.; Fu, W.; Jiang, P.; Zhao, K.; Li, Y.; Penttinen, P. Spatial variability of soil nutrients in forest areas: A case study from subtropical China. *J. Plant Nutr. Soil Sci.* **2018**, *181*, 827–835. [CrossRef]
6. Gruba, P.; Mulder, J.; Pacanowski, P. Combined effects of soil disturbances and tree positions on spatial variability of soil pHCaCl2 under oak and pine stands. *Geoderma* **2020**, *376*, 114537. [CrossRef]
7. Šamonil, P.; Valtera, M.; Bek, S.; Šebková, B.; Vrška, T.; Houška, J. Soil variability through spatial scales in a permanently disturbed natural spruce-fir-beech forest. *Eur. J. For. Res.* **2011**, *130*, 1075–1091. [CrossRef]
8. Phillips, J.D. Soil Complexity and Pedogenesis. *Soil Sci.* **2017**, *182*, 117–127. [CrossRef]
9. Sivakumar, B. Nonlinear dynamics and chaos in hydrologic systems: Latest developments and a look forward. *Stoch. Environ. Res. Risk Assess* **2008**, *23*, 1027–1036. [CrossRef]
10. Turcotte, D.L. *Fractals and Chaos in Geology and Geophysics*, 2nd ed.; Cambridge University Press: New York, NY, USA, 2012.
11. Finke, P.A.; Vanwalleghem, T.; Opolot, E.; Poesen, J.; Deckers, J. Estimating the effect of tree uprooting on variation of soil horizon depth by confronting pedogenetic simulations to measurements in a Belgian loess area. *J. Geophys. Res. Earth Surf.* **2013**, *118*, 2124–2139. [CrossRef]
12. Phillips, J.D. Divergent evolution and the spatial structure of soil landscape variability. *Catena* **2001**, *43*, 101–113. [CrossRef]
13. Phillips, J.D. Soils as extended composite phenotypes. *Geoderma* **2009**, *149*, 143–151. [CrossRef]

14. Šamonil, P.; Egli, M.; Steinert, T.; Norton, K.; Abiven, S.; Daněk, P.; Hort, L.; Brandová, D.; Christl, M.; Tikhomirov, D. Soil denudation rates in an old-growth mountain temperate forest driven by tree uprooting dynamics, Central Europe. *Land Degrad. Dev.* **2020**, *31*, 222–239. [CrossRef]
15. Šamonil, P.; Vašíčková, I.; Daněk, P.; Janík, D.; Adam, D. Disturbances can control fine-scale pedodiversity in old-growth forests: Is the soil evolution theory disturbed as well? *Biogeosciences* **2014**, *11*, 5889–5905. [CrossRef]
16. Daněk, P.; Šamonil, P.; Phillips, J. Geomorphic controls of soil spatial complexity in a primeval mountain forest in the Czech Republic. *Geomorphology* **2016**, *273*, 280–291. [CrossRef]
17. Buurman, P.; Jongmans, A.G. Podzolisation and soil organic matter dynamics. *Geoderma* **2005**, *125*, 71–83. [CrossRef]
18. Anderson, H.A.; Berrow, M.L.; Farmer, V.C.; Hepburn, A.; Russell, J.D.; Walker, A.D. A reassessment of podzol formation processes. *J. Soil Sci.* **1982**, *33*, 125–136. [CrossRef]
19. Wang, C.; Kodama, H. Pedogenic Imogolite in Sandy Brunisols of Eastern Ontario. *Can. J. Soil Sci.* **1986**, *66*, 135–142. [CrossRef]
20. Ditzler, C.; Scheffe, K.; Monger, H.C. (Eds.) Soil science division staff. Soil survey manual. In *USDA Handbook 18*; Government Printing Office: Washington, DC, USA, 1993.
21. Beck, H.E.; Zimmermann, N.E.; McVicar, T.R.; Vergopolan, N.; Berg, A.; Wood, E.F. Present and future Köppen-Geiger climate classification maps at 1-km resolution. *Sci. Data* **2018**, *5*, 180214. [CrossRef]
22. FAO. IUSS Working Group WRB: World Reference Base for Soil Resources, 1998. In *World Soil Resources Reports 84*; FAO: Rome, Italy, 2008; ISBN 978-92-5-305511-1.
23. Food and Agriculture Organization of the United Nations. *World Reference Base for Soil Resources 2014: International Soil Classification System for Naming Soils and Creating Legends for Soil Map*; FAO: Rome, Italy, 2014; ISBN 978-92-5-108369-7.
24. Schoeneberger, P.J.; Wysicki, D.A.; Benham, E.C.; Broderson, W.D. *Field Book for Describing and Sampling Soils*; Natural Resources Conservation Service, USDA, National Soil Survey Center: Lincoln, NE, USA, 1998.
25. Solly, E.F.; Weber, V.; Zimmermann, S.; Walthert, L.; Hagedorn, F.; Schmidt, M.W.I. A Critical Evaluation of the Relationship between the Effective Cation Exchange Capacity and Soil Organic Carbon Content in Swiss Forest Soils. *Front. For. Glob. Chang.* **2020**, *3*, 98. [CrossRef]
26. Lundström, U.S.; Van Breeman, N.; Bain, D. The podzolisation process. A review. *Geoderma* **2000**, *94*, 91–107. [CrossRef]
27. Král, K.; Janík, D.; Vrška, T.; Adam, D.; Hort, L.; Unar, P.; Šamonil, P. Local variability of stand structural features in beech dominated natural forests of Central Europe: Implications for sampling. *For. Ecol. Manag.* **2010**, *260*, 2196–2203. [CrossRef]
28. Nielsen, D.R.; Bouma, J. (Eds.) Soil spatial variability. In Proceedings of the A Workshop of the ISSS and the SSSA, Las Vegas, NV, USA, 30 November–1 December 1984; Pudoc: Wageningen, The Netherlands, 1985.
29. McGrath, D.; Zhang, C.; Carton, O.T. Geostatistical analyses and hazard assessment on soil lead in Silvermines area, Ireland. *Environ. Pollut.* **2004**, *127*, 239–248. [CrossRef] [PubMed]
30. Shapiro, S.S.; Wilk, M.B. An analysis of variance test for normality (complete samples). *Biometrika* **1965**, *52*, 591–611. [CrossRef]
31. Trangmar, B.B.; Yost, R.S.; Uehara, G. Application of Geostatistics to Spatial Studies of Soil Properties. *Adv. Agron.* **1986**, *38*, 45–94.
32. Cressie, N.; Wikle, C.K. The Variance-Based Cross-Variogram: You Can Add Apples and Oranges. *Math. Geol.* **1998**, *30*, 789–799. [CrossRef]
33. Webster, R.; Oliver, M. *Geostatistics for Environmental Scientists Statistics in Practice*; Wiley: Chichester, UK, 2001; p. 271.
34. Minasny, B.; McBratney, A.B. The Matérn function as a general model for soil variograms. *Geoderma* **2005**, *128*, 192–207. [CrossRef]
35. Kalpić, D.; Hlupić, N.; Lovrić, M. Student's t-Tests. In *International Encyclopedia of Statistical Science*; Lovric, M., Ed.; Springer: Berlin/Heidelberg, Germany, 2011.
36. Wilcoxon, F. Individual Comparisons by Ranking Methods. *Biom. Bull.* **1945**, *1*, 80–83. [CrossRef]
37. Zuur, A.; Ieno, E.; Smith, G. *Analysing Ecological Data*; Springer International Publishing: New York, NY, USA, 2007.
38. Borcard, D.; Gillet, F.; Legendre, P. *Numerical Ecology with R*, 2nd ed.; Springer International Publishing: New York, NY, USA, 2018.
39. Jenny, H. *Factors of Soil Formation*; McGraw/Hill: New York, NY, USA, 1941; p. 281.
40. Egli, M.; Dahms, D.; Norton, K. Soil formation rates on silicate parent material in alpine environments: Different approaches–different results? *Geoderma* **2014**, *213*, 320–333. [CrossRef]
41. d'Amico, M.E.; Freppaz, M.; Filippa, G.; Zanini, E. Vegetation influence on soil formation rate in a proglacial chronosequence (Lys Glacier, NW Italian Alps). *Catena* **2014**, *113*, 122–137. [CrossRef]
42. Alewell, C.; Egli, M.; Meusburger, K. An attempt to estimate tolerable soil erosion rates by matching soil formation with denudation in Alpine grasslands. *J. Soils Sediments* **2015**, *15*, 1383–1399. [CrossRef]
43. Román-Sánchez, A.; Laguna, A.; Reimann, T.; Giraldez, J.V.; Peña, A.; Vanwalleghem, T. Bioturbation and erosion rates along the soil-hillslope conveyor belt, part 2: Quantification using an analytical solution of the diffusion–advection equation. *Earth Surf. Process. Landf.* **2019**, *44*, 2066–2080. [CrossRef]
44. Minasny, B.; Finke, P.; Stockmann, U.; Vanwalleghem, T.; McBratney, A. Resolving the integral connection between pedogenesis and landscape evolution. *Earth Sci. Rev.* **2015**, *150*, 102–120. [CrossRef]
45. Boruvka, L.; Mladkova, L.; Drabek, O. Factors controlling spatial distribution of soil acidification and Al forms in forest soils. *J. Inorg. Biochem.* **2005**, *99*, 1796–1806. [CrossRef] [PubMed]
46. Norton, S.A.; Veselý, J. Acidification and Acid Rain. In *Environmental Geochemistry, Treatise on Geochemistry*; Lollar, B.S., Ed.; Elsevier BV: Amsterdam, The Netherlands, 2003; Volume 9, pp. 367–406.

47. Drábek, O.; Mládková, L.; Borůvka, L.; Száková, J.; Nikodem, A.; Němeček, K. Comparison of watersoluble and exchangeable forms of Al in acid forest soils. *J. Inorg. Biochem.* **2005**, *99*, 1788–1795. [CrossRef] [PubMed]
48. Drábek, O.; Borůvka, L.; Pavlů, L.; Nikodem, A.; Pírková, I.; Vacek, O. Grass cover on forest clear-cut areas ameliorates soil chemical properties. *J. Inorg. Biochem.* **2007**, *101*, 1224–1233. [CrossRef]
49. Pritchett, W.L.; Fisher, R.F. *Properties and Management of Forest Soils*, 2nd ed.; John Wiley: New York, NY, USA, 1987; p. 494.
50. Johnson, A.H.; Anderson, S.B.; Siccama, T.G. Acid rain and soils of the Adirondacks. I. Changes in pH and available calcium: Canadian. *J. For. Res.* **1994**, *24*, 193–198.
51. Richter, D.D.; Markewitz, D.; Wells, C.G.; Allen, H.L.; April, R.; Heine, P.R.; Urrego, B. Soil chemical change in an old-field loblolly pine ecosystem. *Ecology* **1994**, *75*, 1463–1473. [CrossRef]
52. Šamonil, P.; Daněk, P.; Schaetzl, R.; Vašíčková, I.; Valtera, M. Soil mixing and genesis as affected by tree uprooting in three temperate forests: Soil mixing and evolution as affected by tree-throw. *Eur. J. Soil Sci.* **2015**, *66*, 589–603. [CrossRef]
53. Boruvka, L.; Mladkova, L.; Penizek, V.; Drabek, O.; Vasat, R. Forest soil acidification assessment using principal component analysis and geostatistics. *Geoderma* **2007**, *140*, 374–382. [CrossRef]
54. Nikodem, A.; Pavlů, L.; Kodešová, R.; Borůvka, L.; Drábek, O. Study of podzolization process under different vegetation cover in the Jizerské hory Mts. region. *Soil Water Res.* **2013**, *8*, 1–12. [CrossRef]
55. Oliveira Rabel, D.; Carlos Vargas Motta, A.; Zimmer Barbosa, J.; Freitas Melo, V.; Arthur Prior, S. Depth distribution of exchangeable aluminum in acid soils: A study from subtropical Brazil. *Acta Sci. Agron.* **2018**, *40*, 39320. [CrossRef]
56. Guajardo, C.; Recio-Espejo, J.M.; Sandoval, M.; Diaz, F.; Bustamente, M.; García-Ferrer, A. Anthropogenic alteration of available, amorphous, and total iron in an Andisol from dairy slurry applications over a 12-year period. *Chil. J. Agric. Res.* **2020**, *80*, 108–117. [CrossRef]
57. Román-Sánchez, A.; Willgoose, G.; Giráldez, J.V.; Peña, A.; Vanwalleghem, T. The effect of fragmentation on the distribution of hillslope rock size and abundance: Insights from contrasting field and model data. *Geoderma* **2019**, *352*, 228–240. [CrossRef]
58. Román-Sánchez, A.; Temme, A.; Willgoose, G.; van den Berg, D.; Gura, C.; Vanwalleghem, T. The fingerprints of weathering: Grain size distribution changes along weathering sequences in different lithologies. *Geoderma* **2021**, *383*, 114753. [CrossRef]